

# Stress-Strain Relationship for the Localized Compressive Failure Zone of Concrete under Cyclic Loading

Ken Watanabe<sup>1)</sup>, Junichiro Niwa<sup>2)</sup>, Hiroshi Yokota<sup>3)</sup>, and Mitsuyasu Iwanami<sup>4)</sup>

*1) Doctoral student, Department of Civil Engineering, Tokyo Institute of Technology, Japan*

*2) Professor, Department of Civil Engineering, Tokyo Institute of Technology, Japan*

*3) Chief research engineer, Structural Mechanics Division, Port and Airport Research Institute, Japan*

*4) Research engineer, Structural Mechanics Division, Port and Airport Research Institute, Japan  
96b31400@cv.titech.ac.jp, jniwa@cv.titech.ac.jp, hiroy@pari.go.jp, iwanami@pari.go.jp*

**Abstract:** To predict the behavior of a concrete structure under seismic loading, the stress-strain curve of concrete in compression is important material characteristic. Current models are including the influence of compressive strength. By the way, the localization of failure of concrete in compression is also influential on the stress-strain curve; hence, the stress-strain curve is strongly changing with the aspect ratio of a concrete specimen. The objective of this study is to establish the hysteresis model of concrete in compression considering the localization and compressive strength of concrete. To overcome the localization of failure, it is assumed that the zone of strain softening (failure zone) of a specimen is coupling in series to “transition zone” and “unloading zone”, such that the stresses carried by these 3 zones are equal and their strains are superimposed with considering the extent of each zone. In this paper, the hysteresis loop model for a failure zone, which governs the overall behavior of concrete structures, was presented in comparison with the experimental loop.

## 1. INTRODUCTION

To predict the behavior of a concrete structure under seismic loading, the model for the stress-strain relationship of concrete under cyclic loading (hysteresis loop) is important material characteristic. Current models (i.e., Karsan and Jirsa 1969) are including various influential factors and experimental conditions on the hysteresis loop. Especially, the influence of compressive strength has been discussed. By the way, Figure 1 shows the failed concrete specimen and stress-strain relationship with diameter  $D$  of 100 mm and varied height  $H$ ; height to diameter ratio  $H/D$  is changing (Watanabe et al. 2003). The localization of failure in compression is clearly observed. And the localization is also influential on the stress-strain relationship; hence, the stress-strain relationship is strongly changing with the aspect ratio of a concrete specimen (Figure 1 (a)). However, the model involving an influence of the localization has not been formulated.

The objective of this study is to establish the hysteresis model of concrete in compression considering the localization and compressive strength of concrete. A series of uniaxial one-directional repeated load test (specimens have been loaded up to the maximum load, then turned to be unloaded) has been conducted with measuring stress-strain relationships (hysteresis loop) at each local portion of the specimen by the acrylic-rod method (the experiment was detailed in section 2). To overcome the localization of failure, it is assumed that the zone of strain softening (failure zone) of a specimen is coupling in series to “transition zone” and “unloading zone”, such that the stresses carried by these 3 zones are equal and their strains are superimposed with considering the extent of each zone (Watanabe et al. 2003). Similar concepts are proposed previously (i.e., a series coupling model, Bazant (1989)). The length of a failure zone was calculated from the cross-sectional area of a concrete specimen (Lertsrisakulrat et al. 2001). Then,

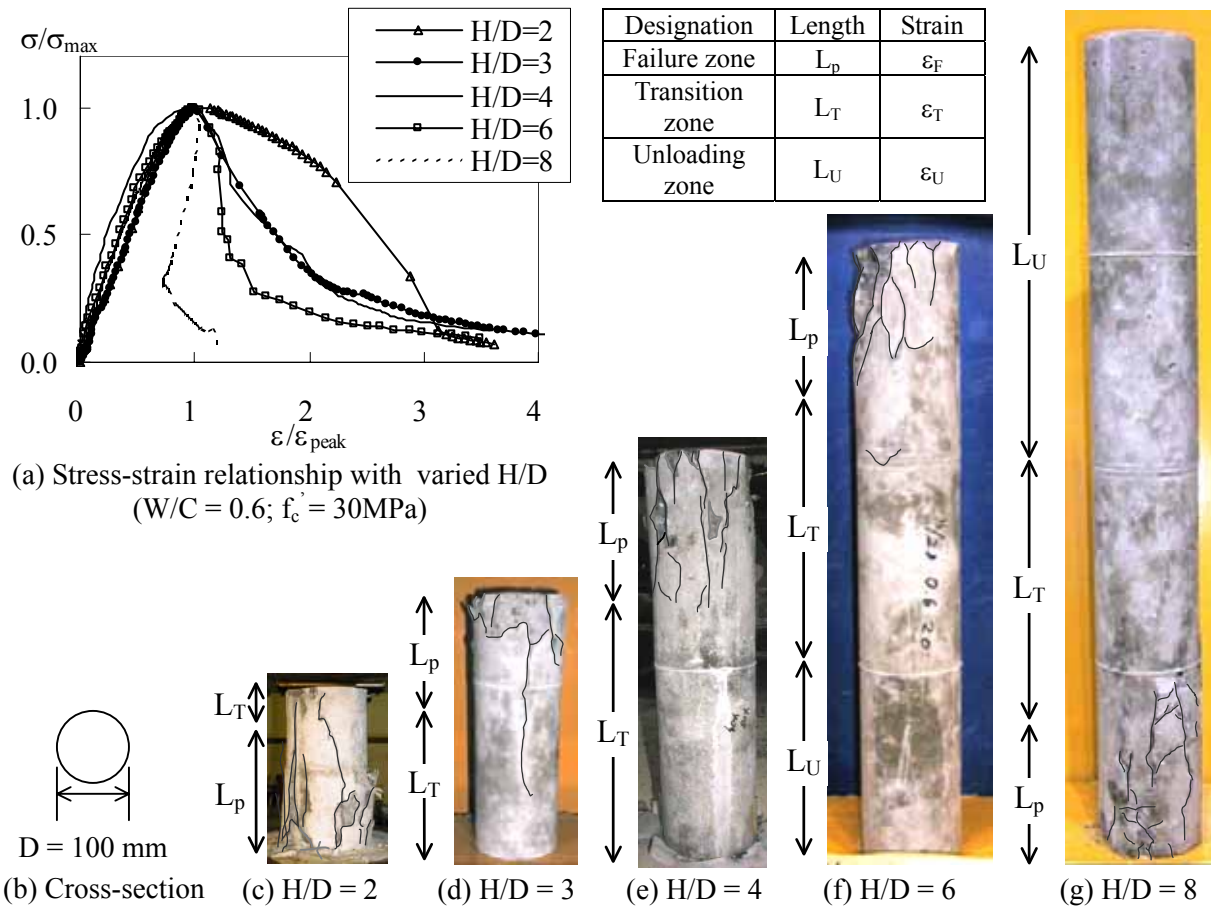


Figure 1 Failed specimen and stress-strain relationship with varied H/D (Watanabe et al. 2003). (black lines indicate crack observed clearly)

the model for an envelope curve involving a characteristic of compressive strength of concrete was formulated for each zone (Watanabe et al. 2003). By combining 3 models considering the extent of each zone, a new model to express an experimental value of envelope curve of the specimen can be obtained regardless the aspect ratio.

Finally, a hysteresis loop model for overall behavior of a concrete specimen with any aspect ratio was established. Each hysteresis loop model for failure, transition and unloading zones was formulated. In this paper, the hysteresis loop model for a failure zone, which governs the overall behavior of concrete structures, was presented in comparison with the experimental loop.

## 2. OUTLINE OF UNIAXIAL COMPRESSIVE TEST

### 2.1 Specimen

Tested specimens are listed in Table 1. Two specimens were used for each case. Cylindrical specimens were made with diameter (D) of 100 mm. To investigate the effect of concrete strength on the hysteresis loop, water-to-cement ratios of concrete are set to 0.4, 0.5, 0.6 and 0.7. Coarse aggregate with the maximum size ( $G_{max}$ ) of 13 mm and 20 mm were used in these specimens. Height of specimens was 400 mm (H/D=4), which indicates the localized failure clearly (Lertsrisakulrat et al. 2001). The compressive strength of concrete ( $f'_c$ ) ranged from 26.2 to 48.4 MPa at the time of test. The value of  $f'_c$  was determined from the standard cylindrical specimen of 200 mm in height and 100 mm in diameter.

Table 1 Tested Specimen.

H/D	$G_{max}$ (mm)	Water to Cement ratio	$f'_c$ (MPa)	$\sigma_{max}$ (MPa)	$L_p$ (mm)	Designation
4	13	0.4	47.3	41.9	120	A13-0.4-4
		0.5	42.0	39.3	120	A13-0.5-4
		0.6	32.2	27.7	120	A13-0.6-4
		0.7	26.2	22.0	160	A13-0.7-4
	20	0.4	48.4	47.5	120	A20-0.4-4
		0.5	39.0	34.9	120	A20-0.5-4
		0.6	36.7	30.7	120	A20-0.6-4
		0.7	28.4	22.5	120	A20-0.7-4

$\sigma_{max}$ : maximum stress,  $L_p$ : the failure zone length.

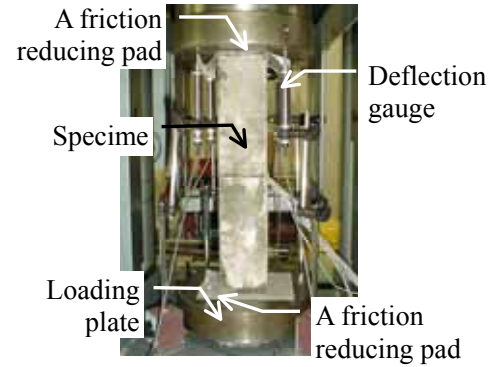


Figure 2 Loading set up.

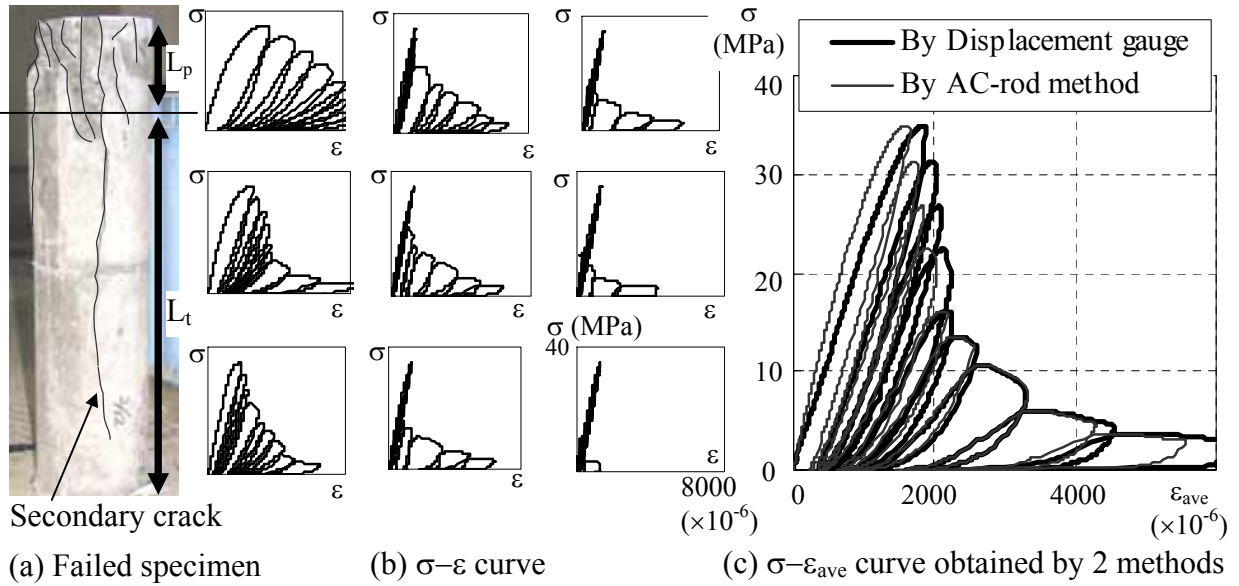


Figure 3 Experimental results (A13-0.5-4).

## 2.2 Loading Test and Measurement

The loading set up is shown in Figure 2. To decrease a friction, friction reducing pads, i.e., two Teflon sheets (0.05 mm thickness) sandwiching silicon grease were inserted between the specimen and loading plates. The specimen was loaded up to the maximum load, then unloaded until 0 kN. With controlled displacement rate of 0.002 mm per second, the load was applied until decreasing to 10% of the maximum load after the peak.

In the loading test, the load ( $P$ ) is measured by a load-cell. The value  $P$  divided by the cross-section area  $A_c$  denotes the stress ( $\sigma$ ). Deformations ( $d$ ) in the specimen were externally measured by deflection gauges, and internal strains were measured by strain gauges (3 mm long) pasted on the acrylic rod with 40 mm interval embedded in the specimen (AC-rod method). The acrylic rod was embedded vertically into a specimen. The strain measured by each gauge denotes a local strain ( $\epsilon$ ), which was assumed to be uniform within 40 mm region of each strain gauge. Average strain ( $\epsilon_{ave}$ ) for the whole of the specimen is obtained by averaging all the value  $\epsilon$  or by dividing the measured value  $d$  with the initial specimen height ( $H$ ).

## 2.3 Experimental Results

The failure mode, a stress-local strain loop ( $\sigma-\epsilon$ ) and a stress-average strain loop ( $\sigma-\epsilon_{ave}$ ) of the specimen A13-0.5-4 are shown in Figure 3. Figure 3(c) suggested that the value  $\epsilon_{ave}$  measured by AC-rod method shows the similar behavior to the strain measured by deflection gauges; hence, a concrete bonded to the acrylic rod and the value  $\epsilon$  can express the strain at the local portion of a

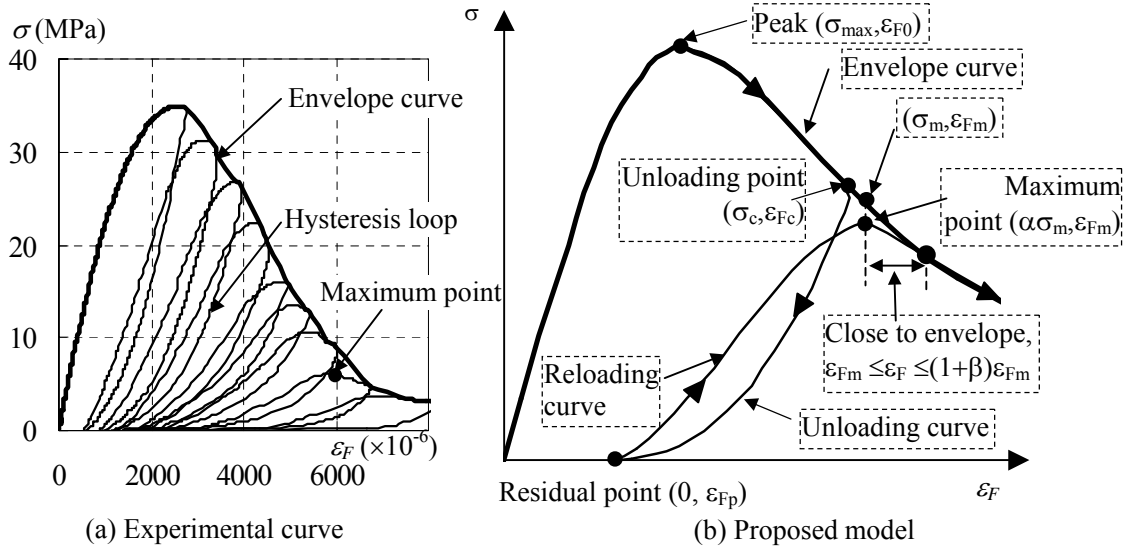


Figure 4 Experimental curve and proposed model of hysteresis loop for the failure zone.

concrete specimen accurately. Based on the existing criterion (Lertsrisakulrat et al. 2001), failed specimens with H/D of 4 are divided into 2 parts; namely a failure zone (length,  $L_p$ ) of the strain softening, and a transition zone (length,  $L_T$ ) where decreasing strain turns to increase in the post-peak region.

### 3. HYSTERESIS LOOP FOR THE FAILURE ZONE

#### 3.1 Definition

Averaging the local strain  $\varepsilon$  measured in the failure zone gives the strain in the failure zone ( $\varepsilon_F$ ). An experimental curve and the proposed model for hysteresis loop in the failure zone ( $\sigma$ - $\varepsilon_F$ ) are shown in Figure 4. The characteristics of the loop are denoted by the following symbol and schematically shown in Figure 4(b). If the value  $\varepsilon_F$  in the post-peak region decreases with the stress ( $\sigma$ ), the traced curve is called an unloading curve ( $\sigma$ - $\varepsilon_{Fu}$ ): between the unloading point ( $\sigma_c, \varepsilon_{Fc}$ ) (a deviation from the envelope curve) and the residual point ( $0, \varepsilon_{Fp}$ ) (the stress reached 0 kN). After completely unloaded, the strain and stress increased again from the residual point, then, approaches to the maximum point ( $\alpha\sigma_m, \varepsilon_{Fm}$ ). The curve is called a reloading curve ( $\sigma$ - $\varepsilon_{Fr}$ ). The locus joining the end of the reloading curve and the start of the unloading curve will be called the envelope curve.

#### 3.2 Envelope Curve

By referring the existing model (Popovics 1973), Watanabe et al. (2003) reported the numerical expression for the envelope curve for the failure zone as follows:

$$\frac{\sigma}{\sigma_{\max}} = \frac{n_F \times \left(\frac{\varepsilon_F}{\varepsilon_{F0}}\right)}{n_F - 1 + \left(\frac{\varepsilon_F}{\varepsilon_{F0}}\right)^{n_F}} \quad (1)$$

where,  $\varepsilon_{F0} = (1.72 \times 10^2 \times \sigma_{\max}^{2/3}) \times 10^{-6}$ ,  $n_F = 3.00 \times 10^{-4} \times \sigma_{\max}^2 + 3.47 \times 10^{-2} \times \sigma_{\max} + 1.86$ .

#### 3.3 Unloading Curve

Figure 5 shows the experimental value and the prediction of the unloading curve; those of the stress and strain are expressed as a ratio between the unloading point and the residual point. At the

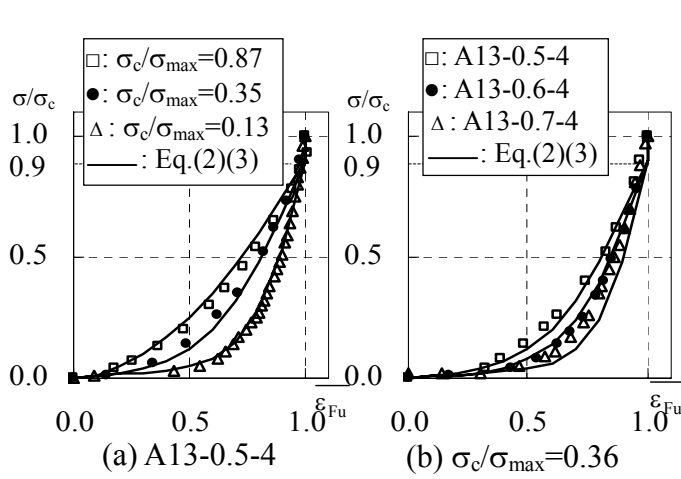


Figure 5 Experimental value and prediction of the unloading curve.

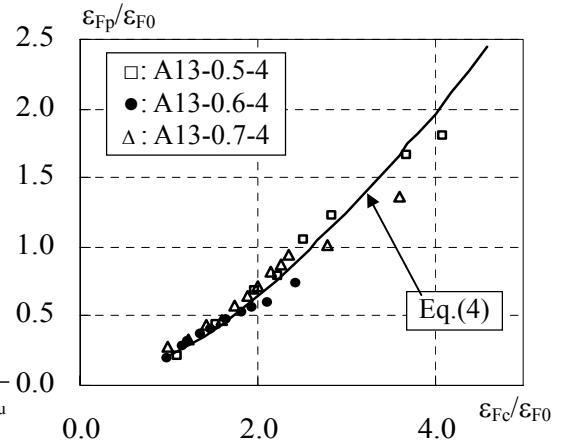


Figure 6  $(\epsilon_{Fc}/\epsilon_{F0})-(\epsilon_{Fp}/\epsilon_{F0})$  relationship.

beginning of unloading, all unloading curves show that the strain ( $\epsilon_{Fc}$ ) is constant during the stress decreasing from  $\sigma_c$  to  $0.9\sigma_c$ . On the other hand, after the point  $(0.9\sigma_c, \epsilon_{Fc})$ , a shape of the convex curve is not unique. As shown in Figure 5(a), a curvature increased with the decrease in the stress at the unloading point ( $\sigma_c$ ). In addition, Figure 5(b) shows that the value  $\sigma_{max}$  also affected the unloading curve, even if the value  $\sigma_c/\sigma_{max}$  of each unloading point is the same.

In traditional empirical equations (Karsan and Jirsa 1969), the convex curve was expressed by using a power function. However, the convex curve near the horizontal axis became flat as the value  $\sigma_c/\sigma_{max}$  decreased. Therefore, it would be difficult to express the experimental results by a single expression. Here, a polynomial expression was adopted as follows:

$$\overline{\epsilon_{Fu}} = 1.0 \quad (0.9\sigma_c \leq \sigma \leq \sigma_c) \quad (2)$$

$$\frac{\sigma}{\sigma_c} = 0.9 \left\{ (\overline{\epsilon_{Fu}})^{u_F} + 0.1 \overline{\epsilon_{Fu}} \left(1 - \frac{\sigma_c}{\sigma_{max}}\right) (1 - \overline{\epsilon_{Fu}})^{0.1} \right\} \quad (0 \leq \overline{\epsilon_{Fu}} \leq 1.0) \quad (3)$$

where,  $\overline{\epsilon_{Fu}} = (\epsilon_F - \epsilon_{Fp}) / (\epsilon_{Fc} - \epsilon_{Fp})$ ,  $u_F = 1.73 \times (\sigma_c/\sigma_{max})^{(-21/\sigma_{max})}$ .

To predict the strain at the residual point, the relationship of the strain between the unloading point ( $\sigma_c, \epsilon_{Fc}$ ) and the residual point ( $0, \epsilon_{Fp}$ ) is plotted in Figure 6. Both strains are divided by the peak strain ( $\epsilon_{F0}$ ). There are slight differences caused by  $\sigma_{max}$ . However, the identical equation could be applied to express the experimental curve. Previous studies (Karsan and Jirsa 1969) argued that the relationship could be predicted by an exponential function or a quadratic function. According to the JSCE (2002), the relationship in Figure 6 is formulated as follows:

$$\epsilon_{Fp} = \epsilon_{Fc} - 2.7\epsilon_{F0} \left( 1 - \exp \left( -0.35 \frac{\epsilon_{Fc}}{\epsilon_{F0}} \right) \right) \quad (4)$$

### 3.4 Reloading Curve

Figure 7 shows the experimental value and the prediction of the reloading curve; those of the stress and strain are expressed as a ratio between the residual point and the maximum point. Figure 7(a), obtained by the specimen A13-0.5-4, indicates that the shape of the unloading curve changes with the strain ratio between the residual point and the peak point ( $\epsilon_{Fp}/\epsilon_{F0}$ ). In addition, Figure 7(b) shows the curve of 3 specimens reloaded from the residual point with the identical  $\epsilon_{Fp}/\epsilon_{F0}$ . It is

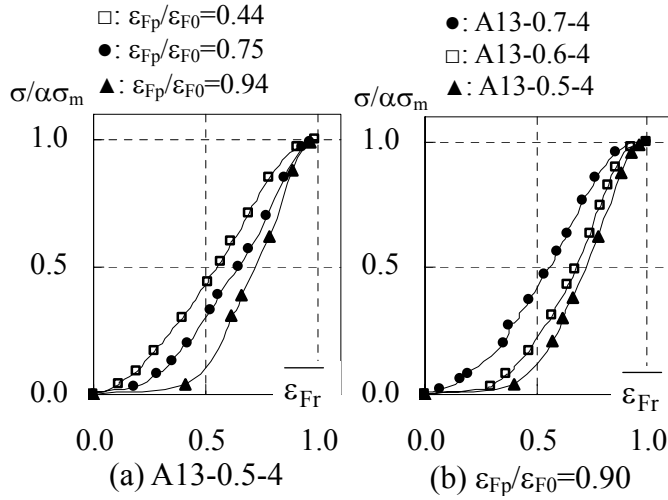


Figure 7 Experimental value and prediction of the reloading curve.

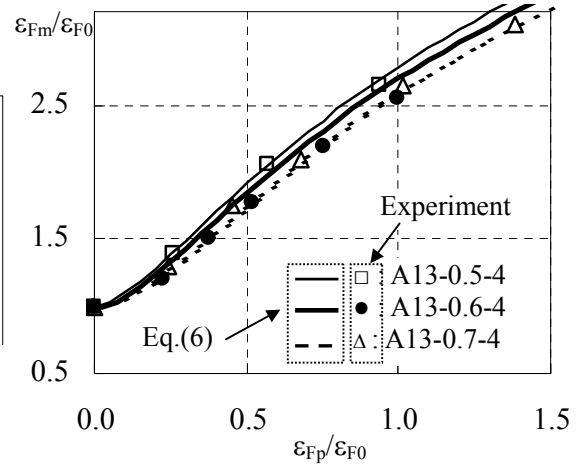


Figure 8  $(\epsilon_{Fp}/\epsilon_{F0}) - (\epsilon_{Fm}/\epsilon_{F0})$  relationship.

clarified that the influence of the value  $\sigma_{max}$  exists on a shape of the reloading curve. Therefore, the reloading model involving  $\sigma_{max}$  and  $\epsilon_{Fp}/\epsilon_{F0}$  should be formulated. Based on Eq. (1), a new value ( $n_{fb}$ ) is added as the power, which is corresponding to the bending degree of the reloading curve. The value  $n_{fb}$  is captured as fitting the calculation by the equation with the experimental curve for each case, and approximated with relation to  $\sigma_{max}$  and  $\epsilon_{Fp}/\epsilon_{F0}$ .

By the way, Figure 4(a) implies that the maximum point  $(\alpha\sigma_m, \epsilon_{Fm})$  does not exist on the envelope curve. A stress of the maximum point is slightly lower than the value  $\sigma_m$ : the stress of the point on the envelope curve and corresponding to the identical strain ( $\epsilon_{Fm}$ ). When cracked concrete is subjected to loading and unloading, the strength of concrete may decrease with closing and opening of cracks. Experimental results indicated that the value  $\alpha$  might depend on  $\sigma_{max}$  and  $\epsilon_{Fp}/\epsilon_{F0}$ .

By summarizing these discussions, the reloading curve from the residual point to the maximum point is formulated as follows:

$$\frac{\sigma}{\sigma_m} = \frac{n_F \left( \frac{\epsilon_{Fr}}{\epsilon_{F0}} \right)^{n_{fb}}}{n_F - 1 + \left( \frac{\epsilon_{Fr}}{\epsilon_{F0}} \right)^{n_F \times n_{fb}}} \times \alpha \quad (5)$$

where,  $\overline{\epsilon_{Fr}} = (\epsilon_F - \epsilon_{Fp}) / (\epsilon_{Fm} - \epsilon_{Fp})$ ,  $n_{fb} = \exp(0.025\sigma_{max}(\epsilon_{Fp}/\epsilon_{F0}))$ ,  $\alpha = 1 - 0.2(\sigma_{max}/50)(\epsilon_{Fp}/\epsilon_{F0})$ .

To predict the strain at the maximum point ( $\epsilon_{Fm}$ ), the relationship between the value  $\epsilon_{Fp}$  and  $\epsilon_{Fm}$  is plotted in Figure 8. By comparing 3 results, there is just a difference depending on  $\sigma_{max}$ . An approximation without the difference is not adequate to express a common point (Karsan and Jirsa 1969). Therefore, each relationship is predicted by the function of  $\sigma_{max}$  as follows:

$$\frac{\epsilon_{Fm}}{\epsilon_{F0}} = a \exp\left(-2b \frac{\epsilon_{Fp}}{\epsilon_{F0}}\right) - (a + 0.8) \exp\left(-b \frac{\epsilon_{Fp}}{\epsilon_{F0}}\right) + c \frac{\epsilon_{Fp}}{\epsilon_{F0}} + 1.8 \quad (6)$$

where,  $a = 6.7 \times 10^{-3} \sigma_{max} + 9.7 \times 10^{-1}$ ,  $b = -2.0 \times 10^{-2} \sigma_{max} + 3.2$ ,  $c = -4.0 \times 10^{-3} \sigma_{max} + 1.2$ .

After the maximum point of the reloading curve, the hysteresis loop is gradually getting close to the envelope curve (Figure 4(a)). To consider the behavior after the reloading curve, the value  $\beta$  is added to Eq.(1) while the strain is  $\epsilon_{Fm}$  to  $(1+\gamma)\epsilon_{Fm}$ . In this range, the value  $\beta$  gradually increases

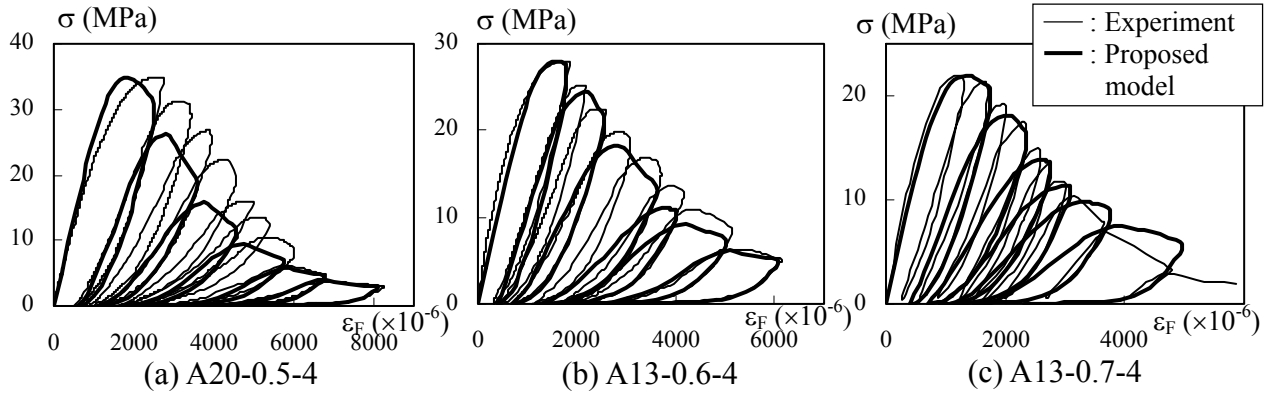


Figure 9 Comparison of proposed model with experimental curve in the failure zone.

from  $\alpha$  to 1. Based on the experimental data, the value  $\gamma$  is decided by the value  $\alpha$  and  $\varepsilon_{Fm}/\varepsilon_{F0}$ : a strain at the maximum point divided by  $\varepsilon_{F0}$ . The equation to express the curve getting close to the envelope curve is formulated as follows:

$$\frac{\sigma}{\sigma_m} = \frac{n_F(\varepsilon_F)}{n_F - 1 + (\varepsilon_F)^{n_F}} \times \beta \quad (\varepsilon_{Fm} \leq \varepsilon_F \leq (1+\gamma)\varepsilon_{Fm}) \quad (7)$$

where,  $\beta = \alpha + (\varepsilon_F - \varepsilon_{Fm})(1-\alpha)/\gamma\varepsilon_{F0}$ ,  $\gamma = 1.4(1-\alpha)(\varepsilon_{Fm}/\varepsilon_{F0})$ .

### 3.5 Comparison of Proposed Model with Experimental Curve

Hysteresis loop in the failure zone ( $\sigma$ - $\varepsilon_F$ ) is predicted by substituting  $\sigma_{max}$  into Eqs. (1) to (7). In Figure 9, the proposed model and experimental results in the failure zone are compared based on  $\sigma_{max}$ . The calculation by the proposed model has a good relation with the experimental curve regardless of  $\sigma_{max}$ .

## 4. CONCLUSION

This paper discusses the hysteresis loop in the localized compressive failure zone of concrete, which governs the behavior for a whole of concrete structure. Then, it is confirmed that the proposed model in this paper can simulate the experimental loop in the failure zone accurately.

### Acknowledgements:

The authors would like to thank ‘Taiheiyō Cement Corporation Research & Development Center’ and ‘Kuraray Co., LTD.’ for their kind supports of the loading test and providing acrylic-rods.

### References:

- Karsan, I.D. and Jirsa, J.O. (1969) “Behavior of Concrete under Compressive Loading,” *Journal of the Structural Division, Proceeding of the American Society of Civil Engineers*, 95(ST12), 2543-2563.
- Watanabe, K., Niwa, J., Yokota, H. and Iwanami, M. (2003) “Formulation of Stress-Strain Relationship of Concrete Considering the Localized Compressive Failure Zone,” *Journal of Materials, Concrete Structures and Pavements*, Japan Society of Civil Engineers, 725/V-58, 197-211.
- Bazant, Z. P. (1989) “Identification of Strain-Softening Constitutive Relation from Uniaxial Tests by Series Coupling Model for Localization,” *Cement and Concrete Research*, 19(6), 973-977.
- Lertsrisakulrat, T., Watanabe, K., Matsuo, M. and Niwa, J. (2001) “Experimental Study on Parameters in Localization of Concrete Subjected to Compression,” *Journal of Materials, Concrete Structures and Pavements*, Japan Society of Civil Engineers, 669/V-50, 309-321.
- Popovics, S. (1973) “A Numerical Approach to the Complete Stress-Strain Curve of Concrete,” *Cement and Concrete Research*, 3(5), 583-599.
- JSCE (2002) “Standard Specifications for Concrete Structures. 2002, Seismic Performance Verification,” Japan Society of Civil Engineers.